Time-dependent analysis of K2PtBr6 binding to lysozyme studied by protein powder and single crystal X-ray analysis

HELLIWELL, John R., BELL, Anthony, BRYANT, P., FISHER, S., HABASH, J., HELLIWELL, Madeleine, MARGIOLAKI, I., KAENKET, S., WATIER, Y., WRIGHT, John P. and YALAMANCHILLI, S.

Published version

HELLIWELL, John R., BELL, Anthony, BRYANT, P., FISHER, S., HABASH, J., HELLIWELL, Madeleine, MARGIOLAKI, I., KAENKET, S., WATIER, Y., WRIGHT, John P. and YALAMANCHILLI, S. (2010). Time-dependent analysis of K2PtBr6 binding to lysozyme studied by protein powder and single crystal X-ray analysis. Zeitschrift fur Kristallographie, 225, 570-575.

Time-dependent analysis of K_2PtBr_6 binding to lysozyme studied by protein powder and single crystal X-ray analysis

John R. Helliwell*, [I], A. M. T. Bell[II, 1], P. Bryant[III], S. Fisher[I, IV], J. Habash[I], Madeleine Helliwell[I], I. Margiolaki[V, VI], S. Kaenket[I], Y. Watier[V], J. Wright[V] and S. Yalamanchilli[I]

[I] School of Chemistry, University of Manchester, UK
[II] STFC Daresbury Laboratory, UK
[III] Life Sciences, University of Manchester, UK
[IV] Institut Laue Langevin, Grenoble, France
[V] ESRF, Grenoble, France
[VI] Department of Biology, University of Patras, Greece

Received September 23, 2010; accepted October 5, 2010

■■■■■■■■■■■■ / ■■■■■■■■■■■■■■■ /
■■■■■■■■■■■■ / ■■■■■■■■■■■■■■■ /

Abstract. Multi heavy atom cluster compounds like K_2PtBr_6 offer a way forward to solve, de novo, unknown protein structures by powder diffraction involving dispersive (measured at two X-ray wavelengths) and isomorphous intensity differences as a complement to micro-crystallography or by using both approaches in combination. Towards this end, using the ESRF high resolution synchrotron X-ray powder diffraction beamline ID31, we have recorded high quality protein powder diffractograms at the platinum LIII and bromine K absorption edges, as well as reference wavelengths, for K_2PtBr_6 bound to lysozyme. These experiments were conducted at 80K to protect the sample against X-radiation damage as much as possible and also to fix the K_2PtBr_6 bound state, which seemed to show instability at room temperature. With multiple powder pattern analysis we extracted intensities and showed the $PtBr_6$ bound in lysozyme using 'omit electron density maps'. In addition the wavelength dispersive Fourier around the Br K edge shows up the bromine signal at $PtBr_6$ binding site 1 in one of the six samples tested. To better understand the chemical properties of this heavy atom compound we have elucidated the detailed binding behaviour using single crystal analyses with time-resolved freeze quenching after soak times of 10, 90 and 170 minutes. Whilst the quick soaking of 10 to 30 minutes, used at ESRF ID31 shows clear binding there is increasing binding strength with increasing soak time. Thus, these time-resolved analytical chemistry results show that further heavy atom signal optimizations are possible. Prospects for extending our approach to the yet larger isomorphous and wavelength dispersive signal case of Ta_6Br_{12} bound to lysozyme are also described.

* Correspondence author
(e-mail: john.helliwell@manchester.ac.uk)
[1] Present address: HASYLAB/DESY, Hamburg, Germany

Introduction

Protein powder diffraction continues to excite strong international interest; there are a variety of applications, including industrial protein characterization, such as polymorphs of insulin, as well as extending structure determination to yet smaller crystal samples, which would otherwise be outside the range of synchrotron X-ray data collection from a protein microcrystal [1–5]. Furthermore there are the upcoming X-ray Laser Facilities, with possibilities for protein nanocluster-crystallites' diffraction and de novo structure determination. There are also both the MWatt spallation and enhanced instrumentation at reactor neutron sources for new powder diffraction opportunities with neutrons as a neutral probe, to complement single crystal studies; the latter are used for specific protein structural studies involving protonation states of titrateable amino acids or H/D exchange dynamics studies, and free of X-ray damage effects. The use of protein powders in neutron work would extend neutron studies to those cases where only smaller crystals can be grown.

Using X-rays, either with MIR [6] or $\Delta f'$ MAD for phasing, it is possible in principle to solve de novo a protein structure from powder diffraction data, even if f'' anomalous differences are not measurable, since the Friedel pairs are overlapped in powder rings, by making use of solvent flattening to 'resolve the inherent phase ambiguity'. To increase the isomorphous or dispersive differences by optimising the heavy atom binding is likely to be important however.

Methods

For the lysozyme powder samples used at ID31 (Supplementary Fig. S1) the soak concentrations were: −10 mM K_2PtBr_6 soaking for ∼10 minutes but could be as long as 30 minutes due to the time needed to fill a capillary including 'centrifuge spin downs'. It was discovered that over a period of up to 12 hours or so the yellow brown of the soaked powder became white again, presumably due

to some type of decay of the K_2PtBr_6. Thus freezing conditions down to 80 K were determined and thereby six powder samples were frozen in 0.8 mm capillaries with an inner cylindrical portion removed so as to facilitate 'low mosaicity increases' by minimising freezing times from the outer to the inner surfaces of the protein powder.

ID31 powder X-ray diffraction data were recorded at the wavelengths of the f' dips and 'soft wavelength remotes' of the Br K edge (respectively 0.9203 Å and 0.9501 Å) with calculated f' values of -8.335 and -3.056 electrons and the Pt LIII edge (1.07245 Å and 1.07331 Å) with f' values from the Kramers Kronig transform, due to white line structure, of -22 to -16 electrons, versus only 2 electrons difference (calculated from [7]). The use of the inflection points as well as remote wavelengths on the soft energy side of each edge sought to maximise $\Delta f'$ whilst minimising absorption changes or stimulation of X-ray fluorescence background as much as possible. At ID31 multiple powder scans, and thereby the use of X-ray radiation damage creating anisotropic changes in unit cell parameters, proved effective in improving the powder data sets' completeness, since the separation and overlap of the powder lines were suitably varied (see Supplementary Fig. S2.)

ID31 was also used to collect high-resolution powder diffraction data on a sample of K_2PtBr_6 *i.e.* without the protein, at ambient temperature. The wavelength settings for the protein powder diffraction measurements were in fact calibrated using this powder sample, at both the platinum LIII and bromine K absorption edges, via its X-ray fluorescence and whereby the f' dip was determined as 1.07245Å versus the tabulated value for a free metal atom of 1.0722Å [7]. This represents an absorption edge shift of -3 eV, *i.e.* in the wrong direction for platinum in oxidation state IV, but which is probably due to the relative rather than absolute angle encoder on the monochromator. Powder X-ray diffraction data were collected at X-ray energies (wavelengths) of 11.58 keV (1.07064 Å), 11.5673 keV (1.07181 Å) and 11.5608 keV (1.07242 Å), *i.e.* close to and at the Pt LIII edge, and these data were used to determine Pt $\Delta f'$ parameters for comparison with those determined for the lysozyme samples. The cif file has been deposited with FIZ with reference code ****.

For the freeze trap time-resolved single crystal evaluations (Supplementary Fig. S3) the following experimental conditions were used: $-11.5/9.4$ mM K_2PtBr_6 19% glycerol for 10 minutes freeze trap 10/8 mM K_2PtBr_6 19% glycerol for 90 minutes freeze trap 10/8 mM K_2PtBr_6 19% glycerol for 170 minutes freeze trap Data collection was carried out on an in house CuK_α rotating anode with RAXIS IV Image Plate (Supplementary Fig. S4). The X-ray diffraction resolution limit was 1.6 Å and the crystal size in each experiment ~0.3 mm. The detailed processed single crystal diffraction data statistics are given in Table 1. The single crystal data sets for the 10, 90 and 170 minutes soaks had good redundancy arising from use of total sweep angles of 180, 360 and 360 degrees with 1 degree oscillations and exposure times of between 2 to 3 minutes per image. These three data sets are of equivalent high quality and very high completeness to 1.8 Å, which is the diffraction resolution to which each of the three protein model refinements were conducted.

Table 1 summarises the protein single-crystal information, data collection and processing statistics and protein final model refinement (in CCP4 REFMAC5) details; the 170 minutes protein model with $PtBr_6$ refined positions are deposited with the PDB as code ****. The use of the refine-

Table 1. Summary of the protein single-crystal information, X-ray data collection and processing statistics and protein final model refinement details.

Parameter	10 minutes	90 minutes	170 minutes
Unit cell dimensions (Å)[a]	$78.74 \times 78.74 \times 36.93$	$78.68 \times 78.68 \times 36.74$	$78.64 \times 78.64 \times 36.45$
Mosaicity (degrees)	1.081	1.837	1.474
Resolution range (Å)	55.68 – 1.63 (1.69 – 1.63)	55.63 – 1.53 (1.59 – 1.53)	55.61 – 1.53 (1.58 – 1.53)
Number of reflections	133628	316122	355325
Number of independent reflections	45933	57644	57600
Redundancy	2.91 (1.27)	5.48 (1.78)	6.17 (1.89)
Completeness	83.0 (15.6)[b]	87.0 (24.7)[c]	87.2 (23.2)[d]
R_{merge}	0.092 (0.309)	0.092 (0.328)	0.081 (0.291)
$\langle I/\mathrm{sig}\ (I)\rangle$	7.0 (1.9)	11.0 (1.6)	12.4 (2.2)
Protein model refinement R_{factor} working set (%)[e]	21.1	20.6	19.8[f]
R_{free} (5% of working set) (%)[e]	27.7	27.0	24.9[f]
N_{ref}	10702	10588	10509
$\langle B\rangle$ (Å^2)	17	19	18
Estimated coordinate uncertainty (Å)	0.17	0.17	0.16

a: Protein crystal system tetragonal and space group $P4_32_12$; data merge made in d*trek (courtesy Dr J. Pflugrath of Rigaku/MSC) in space group $P4$ (I^+ and I^- treated separately).
b: In the resolution shell 1.84–1.76 Å the completeness is 73.7% and at lower resolution basically 100%.
c: In the resolution shell 1.73–1.65 Å the completeness is 88.5%and at lower resolution basically 100%.
d: In the resolution shell 1.72–1.65 Å the completeness is 89.2% and at lower resolution basically 100%.
e: The model refinements used data truncated to 1.8 Å so as to ensure essentially identical data completeness at ~100%.
f: The Protein Data Bank deposition of this, best, final model of the 190 minutes soaked protein crystal structure with bound $PtBr_6$ has PDB code ****.

Table 2. Single crystal occupancy values for the Pt Sites at 10, 90 & 170 minutes soaking at 1.8 Å.

Pt occupancy at Site 1		Pt occupancy at Site 2	Pt occupancy at Site 3
Soak time 10 Minutes	0.33	0.34	0.2
Soak time 90 Minutes	0.39	0.4	0.18
Soak time 170 Minutes	0.5	0.53	0.2

ment program PHENIX provided a quantification of the heavy atom occupancies and these are shown in Table 2 (and Supplementary Fig. S5); the advantage of this approach is that the occupancies are derived from integrated electron density values rather than peak heights and also that the individual bromine atom values can be averaged and yield a spread of values indicative of errors of estimation.

Results

ESRF ID31 yielded high quality protein powder diffractograms from K_2PtBr_6 bound to lysozyme; 80 K temperature was used so as to protect against X-ray radiation damage as much as possible and also to trap *i.e.* fix the K_2PtBr_6 heavy atom compound bound state, which at room temperature showed a change from orange to white over approximately 12 hours and which clearly had to be avoided. With multiple powder pattern analysis we have then extracted individual reflection intensities using the Pawley method [8] and software PRODD [9, 10] and thus been able to show the presence of $PtBr_6^{2-}$ bound in lysozyme in $(Fo - Fc)$ Fourier omit maps, based on calculated phases from the PDB model 1LZ8, at two binding sites (Fig. 1a, which is a close up of binding site 1). The equivalent wavelength dispersive difference Fourier, derived by taking the differences in structure factor amplitudes at the two X-ray wavelengths Br on-edge and Br soft remote, put on a common scale using CCP4 program SCALEIT, for the ID31 data also shows up binding site 1 (at 3.9 sigma) (Fig. 1b). The equivalent dispersive difference Fourier map for the Pt LIII and Pt soft-remote was inconclusive *i.e.* peaks did occur in a cluster close to the binding site 1 but only at 2 sigma. Figure 2 shows a typical PRODD intensity extraction difference plot, this one from data collected on a sample of K_2PtBr_6 bound to lysozyme with 40% glycerol held at 80 K temperature and with an X-ray energy of 11.5516 keV (1.07327 Å) *i.e.* just below the Pt LIII edge at 11.5608 keV (1.0724 Å). This shows the generally very good quality of the extracted powder intensity data that could be obtained. Figure 3 shows a plot of the correlation of structure factor amplitudes for 'sample 4' measured at the soft remote for the Pt LIII edge versus the single crystal observed structure factor amplitudes for the 90 minutes single crystal study; this shows a good correlation certainly to 6 Å resolution *i.e.* 40% or better.

The detailed binding behaviour of this heavy atom compound, was then revealed in more detail via the single crystal analyses with time-resolved freeze quenching after lysozyme single crystal soak times in nearly 10 mM $PtBr_6$ of 10, 90 and 170 minutes. Whilst the quick soaking of 10 to 30 minutes was used in these, our first powder experiments at ESRF ID31, the subsequent time-resolved single crystal characterisation studies show that there is a steady progression of increasing binding strength with in-

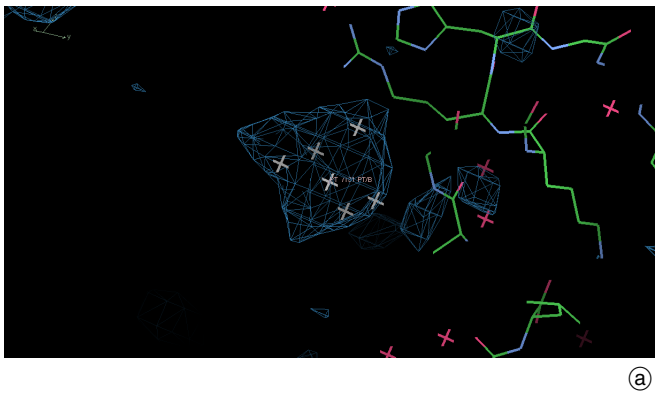

Fig. 1. (**a**) $Fo - Fc$ difference Fourier 3.25 Å electron density map contoured at 2.4σ (blue) and superimposed are the positions of the single crystal 170 minutes study refined Pt and Br positions (Pt is labelled) at site 1, the major site, which is proximal to amino acid residue Arg 14. (**b**) As (a) but with (in yellow) the 3.0σ soft remote minus Br K edge f' dip map (*i.e.* between photon energies respectively of 13.4718 keV and 13.051 keV, *i.e.* wavelengths respectively of 0.9203 Å and 0.95006 Å) from extracted powder diffraction structure amplitudes with calculated phases at 4 Å, which yields a 'dispersive electron density map' illustrated at site 1. The dispersive peak is to the right of the main envelope but very close to a single bromine site and can reasonably be taken to be the all-bromines dispersive signal (the peak height is 3.9 sigma).

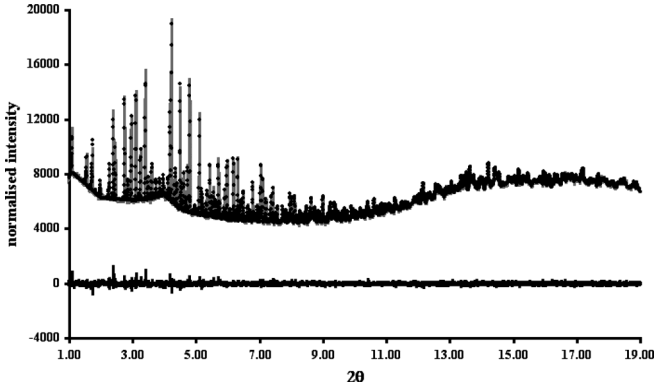

Fig. 2. Intensity extraction from protein powder data. $I(hkl)$ values are variables in a profile fit. Black circles – Observed data. Grey line – Calculated Fit. Black line – Difference (Observed – Calculated). Sample K_2PtBr_6 bound to lysozyme with 40% glycerol, data collected at 80 K and at 11.5516 keV. $R_p = 0.970\%$, $R_{wp} = 1.266\%$, $R_{\rm exp} = 1.0965$, $\chi^2 = 1.3332$.

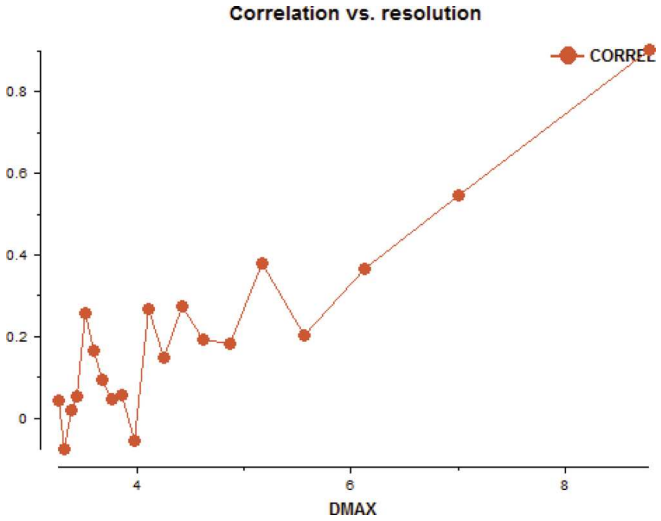

Fig. 3. Correlation between extracted powder structure factor amplitudes for sample 4 ESRF ID31 Pt LIII edge soft remote data and the 90 minutes soaked $PtBr_6$ HEWL single crystal X-ray data. The *x*-axis shows the resolution limit (low resolution to the right and higher resolution to the left). There is a high correlation, around 90% at 8 Å which drops to just under 40% at 6 Å.

creasing soak time (Table 2 and Supplementary Fig. S5) and some further optimisation of the binding occupancy of this compound is possible in any future powder diffraction experiment. The single crystal experiments yielded electron density difference map peak heights which also quantify a steady increase in binding strength (Figs. 4 a, b and c); binding site 1 increasing from 23 to 30 to 35 sigma for 10, 90 and 170 minutes soaking times respectively .

The ID31 powder data isomorphous difference Fourier protein rigid-body model refinement omit maps are encouraging showing consistent heavy atom binding behaviour in all our ID31 samples. A variation in diffraction resolution was seen however with the best being 3.25 Å resolution. The comparison of the single crystal HEWL $PtBr_6$ diffraction amplitudes with the extracted powder data for one example of the HEWL $PtBr_6$ samples (sample number 4) shows that via CCP4 SCALEIT the $R_{\rm factor}$ on F rises from 15% at very low resolution up to 40% at 6 Å and seems to assume near random values upto 3.2 Å *i.e.* around 50%. The REFMAC5 rigid body refinement for sample 4 soft remote powder extracted structure factor amplitudes against the HEWL model (1LZ8), for example, gives an overall $R_{\rm factor}$ of 53%, which is relatively high but in a range adequate for starting molecular replacement; it yielded calculated phases capable of showing the two main binding sites from these extracted powder data.

The K_2PtBr_6 powder diffraction data could be indexed as a single-phase structure with a lattice parameter close to the $Fm\bar{3}m$ structure of K_2PtBr_6 [11]. Figure 5 shows a plot of the K_2PtBr_6 powder diffraction data collected at the 3 different energies at and around the Pt LIII edge on ID31. Note the difference in relative intensities of some Bragg reflections due to the resonant scattering effects. A multi-wavelength Rietveld [12] refinement was done using GSAS [13]. Resonant scattering parameters were determined using GSAS program FPRIME. The $Fm\bar{3}m$ structure of K_2PtBr_6 was used as a starting model for this refinement. Isotropic temperature factors were also refined

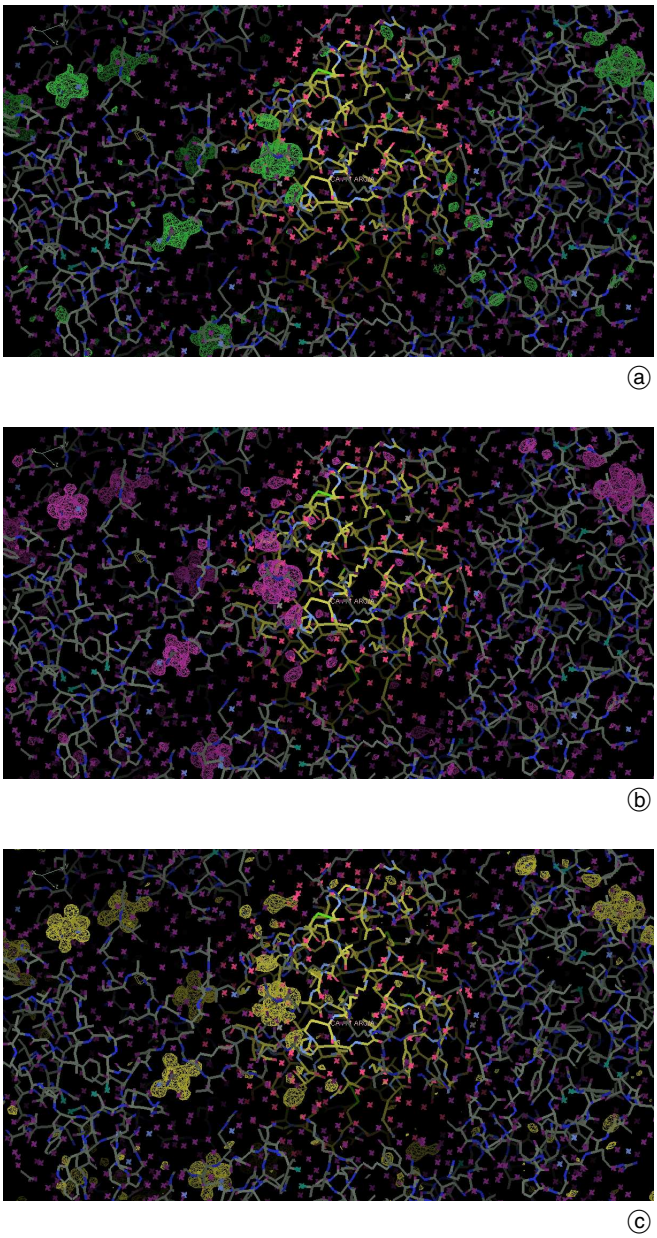

Fig. 4. Single crystal freeze-quench $Fo - Fc$ electron density difference Fourier maps after REFMAC5 rigid body refinement at 1.8 Å resolution (each map contoured at 3σ). The steady progression of improved definition for each binding site of the $PtBr_6$ is self evident as a function of soak times of (**a**) 10 minutes (top), (**b**) 90 minutes (middle) and (**c**) 170 minutes (bottom). [Identical view in each case.]

for K and Br. The temperature factor for Pt could not be refined to a sensible positive value so this was fixed at the value in Ref. [11]. Pt f' parameters were refined for each of the three X-ray energies. Refined structural parameters for K_2PtBr_6 are given in Table 3. Figure 6 shows the Rietveld fit for data collected with an example X-ray energy (11.5608 keV). These show reasonable agreement for the derived f' values with those expected from theory [7]; possible improvements might accrue from starting values of f', f'' obtained from CHOOCH [14] for each wavelength and then refined in GSAS. Such a detailed investigation is outside the scope of this paper but would take account of the stereochemical restraints used in GSAS and where similar studies to be used as examples are [15, 16].

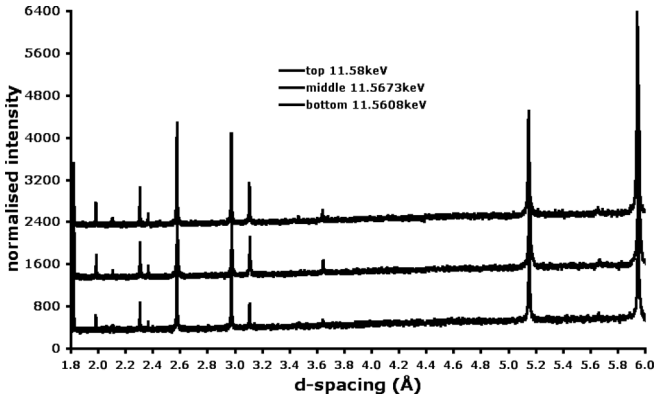

Fig. 5. Normalised X-ray powder diffraction data on K_2PtBr_6 (*i.e.* without protein) collected at different X-ray energies at and near to the Pt LIII edge; note the relative changes of intensities as a function of photon energy.

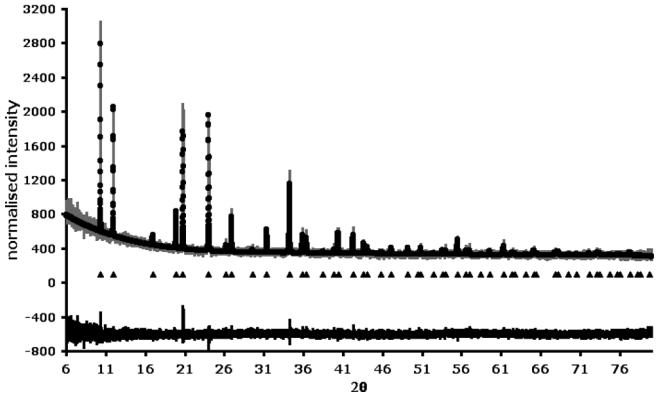

Fig. 6. Rietveld difference plots for K_2PtBr_6 with an X-ray energy of 11.5608 keV. Black circles are observed data points, grey lines are the calculated curve, black lines are the difference curve and black triangles indicate the positions of K_2PtBr_6 Bragg reflections.

Table 3. Refined $Fm\bar{3}m$ structural parameters for K_2PtBr_6. K *xyz* coordinates = 0.25, Pt *xyz* coordinates and Br *yz* coordinates = 0.0, *i.e.* all special positions and not refined.

a (Å)	10.30536(5)
Br x	0.2370(1)
K U_{iso} (Å^2)	0.044(2)
Pt U_{iso} (Å^2) fixed value	0.0090
Br U_{iso} (Å^2)	0.0100(4)
Pt−Br distance (Å)	2.442(1)
K−Br distance (Å)	3.64576(5)
Br−Pt−Br angles (°)	90, 180
Pt f' (electrons) 11.58 keV	−13.3(3)
Pt f' (electrons) 11.5608 keV	−21.9(4)
Pt f' (electrons) 11.5673 keV	−11.2(3)
W_{Rp}	0.0505
R_p	0.0415
χ^2	1.160

Conclusions

The protein powder X-ray diffraction experiments on the lysozyme with bound K_2PtBr_6 have established various experimental factors. We have been able to show that consistent isomorphous binding of the K_2PtBr_6 compound, as monitored by the extracted powder intensity data, has been achieved wavelength dispersive intensity differences around the bromine K edge are evident and led to chemically reasonable difference electron density 'omit maps', but so far only for one sample of the two studied at that absorption edge; this is probably due to variabilities of soaking the K_2PtBr_6, which we have investigated subsequently with the freeze trap single crystal studies the powder work further confirms the high quality of data from ESRF ID31 and of the utility of the intensity extraction procedures notably involving anisotropic cell parameter variation to move the intensities slightly in Bragg angle, but as well confirms the wavelength setting procedures are precise and reproduceable.

We seek a further derivative (lysozyme with Ta_6Br_{12}) to then embark on difference Patterson and de novo phasing analyses, either within and/or between data sets. The single crystal time-resolved analytical chemistry results show that further heavy atom signal optimizations, and reproducible behaviour, are possible for improved protein powder diffraction experiments with the K_2PtBr_6 compound. The crystal structure of K_2PtBr_6 has also been refined from ID31 high-resolution synchrotron X-ray powder diffraction data recorded at three wavelengths and has usefully guided the protein powder multiple wavelength isomorphous and dispersive experiments on lysozyme with bound $PtBr_6$. We will soon be extending our approach to the yet larger isomorphous and wavelength dispersive signal case of Ta_6Br_{12} bound to lysozyme for powder experiments on ESRF ID31.

Overall, such multi heavy atom cluster compounds like K_2PtBr_6 and Ta_6Br_{12} offer a way forward to solve de novo unknown protein structures by powder diffraction as a complement to micro-crystallography or by using both approaches in combination. With such an interesting focus for their application in such challenging experiments of de novo protein structure determination of the type described here these particular heavy atom coordination compounds could usefully be investigated in more detail with respect to their X-ray radiation damage sensitivity, which we are also now studying in detail (to be published).

Acknowledgments. We are grateful to ESRF for the provision of beamtime on ID31 and to the University of Manchester for general support. We thank Dr. Andy Fitch for help and encouragement. We wish to acknowledge the use of the EPSRC Chemical Database Service at Daresbury [17].

References

[1] I. Margiolaki, J. P. Wright, Acta Cryst. 2008, A64, 169–180.
[2] J.R. Helliwell, M. Helliwell, R.H. Jones, Acta Cryst. 2005, A61, 568–574.
[3] B. Hedman, K.O. Hodgson, J.R. Helliwell, R. Liddington, M.Z. Papiz, PNAS, 1985, 82, 7604–7607
[4] J.P. Wright, C. Besnard, I. Margiolaki, S. Basso, F. Camus, A. N. Fitch, G. Fox, P. Pattison, M. Schiltz, J. Appl. Cryst. 2008, 41, 329–339.
[5] I. Collings, Y. Watier, M. Giffard, S. Dagogo, R. Kahn, F. Bonneté, J. P. Wright, A. N. Fitch, I. Margiolaki, Acta Cryst. 2010, D66, 539–48.
[6] S. Basso, C. Besnard, J. P. Wright, I. Margiolaki, A. N. Fitch, P. Pattison, M. Sciltz, Acta Cryst. 2010, D66, 756–761.

[7] S. Sasaki, KEK Report 83–22. National Laboratory for High Energy Physics, Tsukuba, Japan. 1984.
[8] G. S. Pawley, J. Appl. Cryst. 14, 1981, 357–361.
[9] J.P. Wright, J. B. F. Forsyth, Report RAL-TR-2000-012. Rutherford Appleton Laboratory, 2000.
[10] J.P. Wright, Z. Kristallogr. 2004, 219, 791–802.
[11] H.D. Grundy, I.D. Brown. Canadian Journal of Chemistry, 1970, 48, 1151–1154.
[12] H.M. Rietveld. J. Appl. Cryst., 2, 1969, 65–71.
[13] A.C. Larson, R.B. von Dreele. General Structure Analysis System (GSAS), Report LAUR 86-748, Los Alamos National Laboratory. 2004.
[14] G. Evans, R. F. Pettifer J. Appl. Cryst. 2001, 34, 82–86.
[15] I. Margiolaki, J. Wright, M. Wilmanns, A. Fitch, N. Pinotsis, J. Am. Chem. Soc., 129, 2007, 11865–11871.;
[16] S. Basso, A. N. Fitch, G. C. Fox, I. Margiolaki, J. P. Wright. Acta Cryst., D61, 2005, 1612–1625.
[17] D.A. Fletcher, R.F. McMeeking, D.J. Parkin, Chem. Inf. Comput. Sci. 36, 1996, 746–749.

Supplementary Material

Figure S1. The HEWL powder samples soaked in K_2PtBr_6 loaded into kapton capillaries

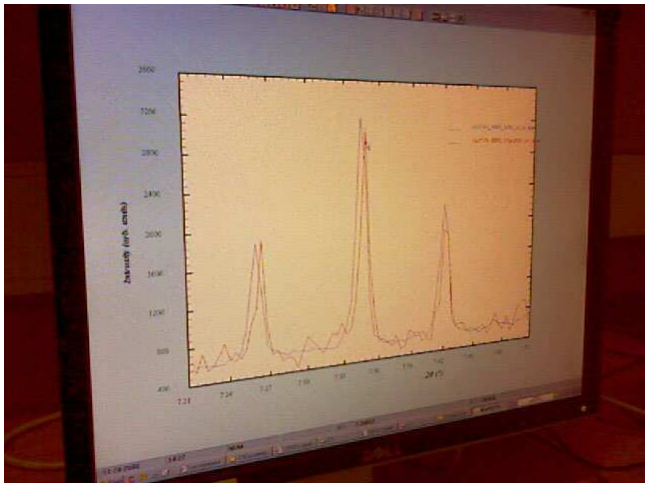

Figure S2. Plot showing the shift in the protein powder diffraction lines due to radiation damage.

Figure S3. Single crystals of hen egg white lysozyme after soaking in $PtBr_6$ solution showing thereby, in the e-version of this figure, a yellow/orange colour. Typical crystal size 0.2 to 0.3 mm.

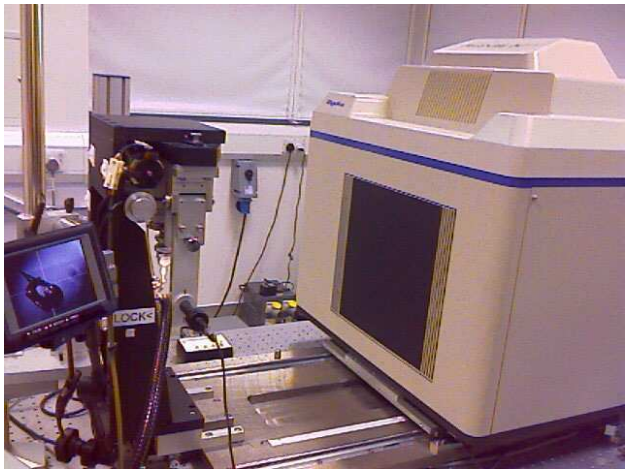

Figure S4. The local RAXIS IV single crystal image plate diffractometer running on a Rigaku rotating anode at CuK_α wavelength.

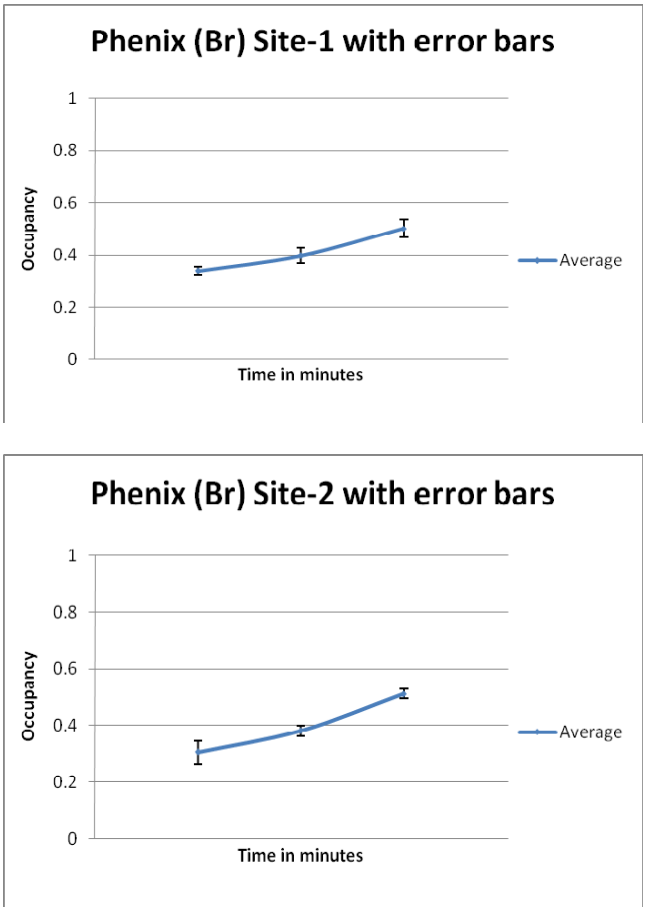

Figure S5. Graph of occupancy values for (a) average of the six Br atoms at Site-1 and (b) average of the six Br atoms at Site 2 in the 10, 90 and170 minutes soak cases with the single crystal diffraction data truncated at 1.8 Å resolution to ensure uniform data quality and completeness values as much as possible. This averaging across the six bromine sites per platinum atom usefully gives a spread of values therefore indicative of the errors of determination of the occupancy although may include a natural spread of values eg due to slightly different mobilities of the bromine atom sites on any one platinum atom and a possible difference in sensitivity of axial versus square planar bomines to X-ray radiation damage within the actual recording of a data set. [This possibility of radiation sensitivity is being investigated separately in our most recent evaluations and characterisation experiments of this heavy atom compound (to be published).]. The site 3 estimates of such a spread of values is unlikely to be useful due to too low an occupancy (~20%) in the first place and is not shown.